DISTRIBUTION OF WATER AND ELECTROLYTE BETWEEN HOMOIONIC CLAYS AND SATURATING NaCl SOLUTIONS

by

FABIAN BERNSTEIN

Schlumberger Well Surveying Corporation, Ridgefield, Connecticut

ABSTRACT

Ion and water uptake from solution by the sodium and hydrogen forms of montmoril-lonite and illite were measured. The clays first were converted to homoionic form by treatment with synthetic ion exchange resins. The hydrogen clays were used to determine the acid strength of the exchange groups by titration with sodium hydroxide solutions. The sodium clays were used to obtain the ion and water distribution. After attainment of equilibrium with sodium chloride solutions, the sodium clays were centrifuged to constant weight and the equilibrating solutions analyzed for NaCl. Ion and water uptake and fixed charge concentration in the clays were then measured.

The clay minerals were found to behave as weak acids and the exchange sites are not appreciably dissociated until the pH of the external solution becomes moderately high. In the sodium form, the exchange sites are fully dissociated and the clays, particularly montmorillonite, become efficient Donnan membranes. The partially neutralized clays exhibit intermediate membrane behavior.

At low external phase salinities, the leakage of anions into the clay solution phase is abnormally large, but the membrane activity remains high because of the low activity coefficients of the diffusible ions in the clay phase. At high external solution salinities, the deswelling of the clays and the decrease in the anion to cation mobility ratio partially compensate for the increased anion leakage.

The abnormally low activities of the diffusible ions are directly related to the effect of the internal phase double layer. The concept of ion retardation in the double layer is used to explain the fact that ion transference numbers computed from internal phase ion concentrations are lower than experimental transference numbers.

The relationship of the electrochemical properties of clays to oil-well log interpretation is briefly discussed.

INTRODUCTION

The cation-exchange properties of clays have long been recognized. The discovery of cation exchange in soils is credited to Thompson (1850) and was confirmed by Way (1850) in the same year. Since then, the exchange process has been studied extensively despite the complexity of clay systems. The introduction of synthetic organic exchange resins in the past 25 years has further advanced the knowledge of natural ion-exchange materials.

It is well known that the ability of a solid, insoluble substance to exchange ions is a consequence of the fixed ionic charges in the solid matrix. A cation exchanger thus can be considered as an insoluble polyanion or polyacid containing diffusible cations (electroneutrality is, of course, observed) which can

122

be exchanged for other cations. When a clay is immersed in water, two solution phases are formed: the saturating solution phase and an internal solution phase, the latter being strongly influenced by the fixed charges of the exchanger.

The equilibrium distribution of water and ions between the two phases was formulated quantitatively by Donnan (1924). The Donnan distribution is shown diagrammatically in Fig. 1 for a homoionic sodium clay (i.e. a clay
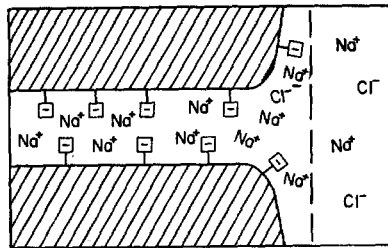

FIGURE 1.—Diagrammatic distribution of Na+ and Cl− ions between internal homoionic Na-clay phase and external NaCl solution. Fixed negative cahrges are denoted by squares attached to clay surfaces.

in which the fixed negative charges are countered by Na+ ions only) immersed in NaCl solution. The fixed negative charges are represented as squares attached to the surface or pore walls of the clay particles. The saturating NaCl solution is shown to the right of the dashed line. The line thus can be taken as a semipermeable membrane separating the internal and external solution phases. Water and Na+ and Cl− ions can diffuse through the membrane; the fixed negative charges are restricted to the internal phase. The amount of water imbibed by the clay depends on its swelling properties which in turn are affected by the salinity of the saturating solution.

At equilibrium, the chemical potentials of NaCl in the two phases are equal, or

$$\bar{\mu}_{NaCl} = \mu_{NaCl} \tag{1}$$

where the barred quantity refers to the internal solution phase and the unbarred quantity to the external solution phase.

It immediately follows from equation (1) that

$$\bar{m}_{Na}\bar{m}_{Cl}\bar{\gamma}^{\pm 2} = m^2\gamma^{\pm 2} \tag{2}$$

where the $\gamma^\pm$'s are the mean molal activity coefficients, and $m = m_{Na} = m_{Cl}$, the molal concentrations.

Since electroneutrality must be observed, in the clay phase

$$\bar{m}_{Na} = A + \bar{m}_{Cl} \tag{3}$$

where A is the molality of the fixed negative charges, viz. the equivalents of fixed charges per kg of water in the internal solution phase.

Substituting equation (3) in (2) gives

$$\bar{m}_{Cl}(\bar{m}_{Cl}+A)\bar{\gamma}^{\pm 2} = m^2\gamma^{\pm 2} \tag{4}$$

or

$$\bar{m}_{Na}(\bar{m}_{Na}-A)\bar{\gamma}^{\pm 2} = m^2\gamma^{\pm 2}. \tag{4a}$$

The individual diffusible ion molalities in the clay phase are obtained by solving the quadratic equations (4) and (4a) to give

$$\bar{m}_{Cl} = \frac{-A+\sqrt{A^2+4m^2(\gamma^{\pm}/\bar{\gamma}^{\pm})^2}}{2} \tag{5}$$

and

$$\bar{m}_{Na} = \frac{A+\sqrt{A^2+4m^2(\gamma^{\pm}/\bar{\gamma}^{\pm})^2}}{2}. \tag{5a}$$

The chief feature of the Donnan equilibrium is the exclusion of anions from the internal solution phase. This property, variously called the Donnan effect, the fixed charge effect, or membrane activity, clearly depends on the fixed charge concentration A. Thus an ideal cation exchanger or membrane will exclude anions completely regardless of the salinity of the saturating solution. As A increases $\bar{m}_{Cl}$ approaches zero and $\bar{m}_{Na}$ approaches A. In the borehole of an oil well, for example, a thick compacted shale bed commonly behaves as an ideal membrane. If both the connate water in an adjacent sand and the mud filtrate in the borehole are taken as NaCl solutions, the system

<p style="text-align:center">mud filtrate (a_{mf})/shale/connate water (a_w)</p>

becomes a sodium concentration cell with a potential in millivolts at 25°C, given by

$$E_m = -59 \log\left(\frac{a_w}{a_{mf}}\right)_{Na^+} \tag{6}$$

where a_w and a_{mf} are the molal activities of Na^+ ion in the connate water and mud filtrate, respectively, and E_m is the ideal membrane potential. In effect, any moderate current through the membrane is carried only by the Na^+ ion.

The electrochemical origin of the spontaneous potential (SP) in the mud-filled borehole of an oil well is shown diagrammatically in Fig. 2. The heavy line opposite the sand bed represents the mud cake, resulting from the excess pressure maintained on the mud column, through which the mud filtrate invades the permeable sand to a distance denoted by the wavy line. The current i is carried through the shale membrane by Na^+ ion only. Through the liquid junction formed by the invading mud filtrate and the connate water, the current is carried by both Cl^- and Na^+ ion.

As will be shown below, the liquid junction coefficient (12 mv) is determined by the relatively higher mobility of Cl^- ion with respect to Na^+ ion.

In a less than ideal exchanger, the Donnan effect is progressively swamped out by increasing the NaCl concentration in the external solution. In the

limiting case of high salinity and low A value, the two solution phases become virtually identical.

The purpose of the present work was to study the effect of salinity on the membrane activity of representative clay minerals. Homoionic samples of montmorillonite and illite were prepared for this purpose. The distribution of ions and water between the clay and external phase was determined as a
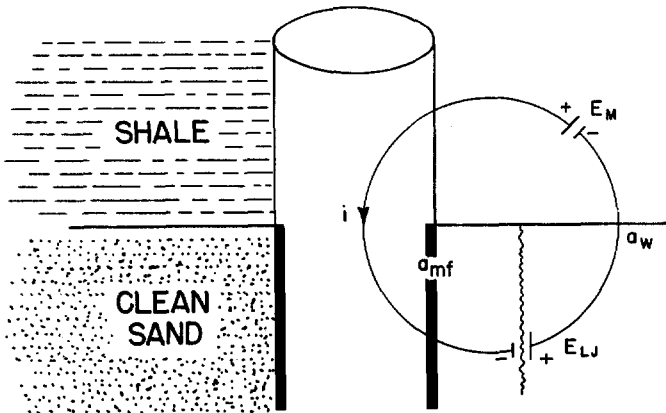

FIGURE 2.—Schematic representation of source of electrochemical SP in mud-filled bore hole of oil well.

$$\text{Electrochemical } SP = E_M + E_{LJ}$$

$$E_M = -59 \log \frac{a_w}{a_{mf}}$$

$$E_{LJ} = 12 \log \frac{a_{mf}}{a_w}$$

$$E_M + E_{LJ} = -71 \log \frac{a_w}{a_{mf}}$$

function of the salinity of the saturating solution. Also, since the dissociation of the polyacid might vary with pH (if the acid is weak), a corollary purpose was to study the acid strength of the clay polyanion and to determine the ion distribution as a function of the degree of neutralization of H-clays.

EXPERIMENTAL TECHNIQUES

Preparation of Homoionic Clays

The homoionic sodium and hydrogen forms of illite and montmorillonite were prepared with the use of three Rohm and Haas Co. ion-exchange resins:

Amberlite IRC-50, IR-120 and IRA-400. The approximate exchange capacities of these resins are 1000, 430 and 300 meq/100 g, respectively. Before use, the resin was conditioned, i.e. treated successively with large excesses of NaOH and HCl until the effluent was free of colored or suspended matter. Finally, the resins were converted to the desired state and washed with deionized water.

A schematic flow sheet of the ion-exchange preparation is shown in Fig. 3. The detailed procedure for preparing the homoionic clays was as follows.
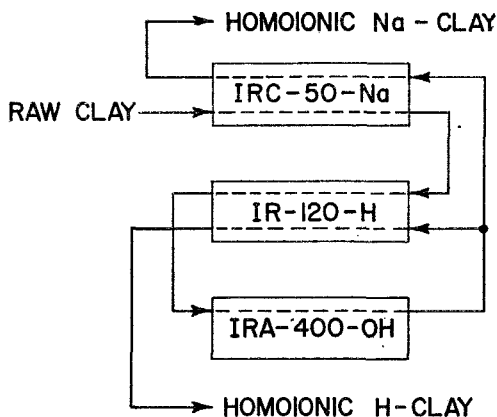

FIGURE 3.—Schematic procedure (flow sheet) for preparation of homoionic clays by ion-exchange column technique.

A slurry of ground illite (API no. 35, Fithian, Illinois, Ward's Natural Science Est.) was prepared with deionized water. The pH was adjusted to 9.0 with the addition of NaOH and the slurry was cycled through an ion-exchange column charged with Amberlite IRC-50-Na form. Regeneration of this column indicated exchange of Mg, Ca and Fe. The slurry then was de-salted by successive cycling through columns charged with Amberlite IR-120-H form and IR-400-OH form, respectively. Regeneration of the IR-120-H column showed additional exchange of iron. The exchange process was continued until a Versene test for Ca, Mg was negative. A portion of the slurry was then passed through a freshly regenerated IRC-50-Na column to prepare the sodium illite. Another portion was passed through the IR-120-H column to prepare the hydrogen illite. All columns were wound with heating tapes to maintain the temperature at approximately 50°C.

Portions of both clay samples were treated with concentrated ammonium acetate and centrifuged. The H-illite filtrate gave a negative test for sodium in the flame photometer. KCNS tests on the filtrates indicated that the iron content of each sample was less than 3 ppm. The slurries were then dried to

constant weight at 50°C in a forced-draft oven. After a final grind, the clay particles passing through a no. 35 Tylor screen were collected and stored in tightly-stoppered amber bottles.

The preparation of homoionic montmorillonite (no. 31, Cameron, Arizona, Ward's Natural Science Est.) was essentially the same except that the initial treatment with IRC-50-Na was replaced by successive washings and decantations, first with concentrated NaCl solution and then with dilute HCl (0.05 N) to reduce the (Ca+Mg) content.

Two additional samples, illite (no. 35, see above) and montmorillonite (no. 30a, Bayard, N. M., Ward's Natural Science Est.) were prepared by repeated washing with 1 N NaOH and 1 N HCl. Only the hydrogen form of these samples was prepared. After a final treatment with HCl, the clays were washed in a Buchner funnel to a Cl⁻-free effluent.

The clays prepared and studied in this work were designated as: (1) H-illite no. 35 (resin); (2) Na-illite no. 35 (resin); (3) H-montmorillonite no. 31 (resin); (4) Na-montmorillonite no. 31 (resin); (5) H-illite no. 35 (acid); and (6) H-montmorillonite no. 30a (acid).

Base Exchange Capacity

Exchange capacities were determined by the API ammonium acetate method (Lewis, 1950), modified to provide for washing of the ammonium clay with ethanol until the effluent was acetate-free. The base exchange capacities of the homoionic clay samples were 25, 77, 13 and 56 meq/100 g for illite no. 35 (resin), montmorillonite no. 31 (resin), illite no. 35 (acid) and montmorillonite no. 30a (acid), respectively.

Analyses

Acid-base titrations were carried out to a phenolphthalein endpoint. A small excess of HCl was added and the titration solution was gently boiled in a tilted Erlenmeyer flask. The solution was then quickly cooled and back-titrated with NaOH.

Chloride ion in solution was determined potentiometrically by titration with $AgNO_3$. The silver electrode was prepared by potting a silver rod in glass tubing with epoxy resin. A fresh silver surface thus could be readily provided for each titration by abrading the tip of the electrode. The potential of the silver electrode was measured with reference to a saturated calomel electrode. To avoid contamination of the test solutions and the salt bridge, the following chain was employed:

Ag/unknown Cl⁻ solution//Agar bridge

(13 percent KNO_3)//KNO_3 (13 percent)//Agar bridge

(sat. KCL)//KCl (sat.)/Hg_2Cl_2/Hg.

For determining Cl⁻ ion uptake by the clays, the centrifuged samples were taken up in distilled water after a quick rinse of the clay cake surface with

2.00 ml of water. The slurry was made acidic by addition of a few drops of nitric acid and then titrated with $AgNO_3$. Just before the endpoint was reached the titration mixture was brought to a gentle boil for 5 min, quickly cooled, and then titrated to the endpoint.

Titration of H-Clays

The H-montmorillonite no. 30a (acid) sample was titrated both in the presence and absence of 1 molal NaCl. Approximately 10-g samples of the clay were taken up in 100 ml water and in 100 ml of 1.0 m NaCl solution, respectively. The NaCl slurry was titrated with standard NaOH made up to be 1 molal with respect to NaCl; the water slurry was titrated with NaOH only. After each addition of base the slurries were stirred for a minimum of 24 hr. The clay particles then were allowed to settle and the pH of the supernatant liquid was measured with a Beckman Model G pH meter.

In the titration of H-illite 35 (resin) and H-montmorillonite 31 (resin), 5-g samples of each clay were weighed into 1×4 in. polythene test tubes. Exactly 25.00 ml of solution was added to each tube. Two series of NaOH solutions were used. One series consisted of NaOH solutions of varying strength; the other was similar but each solution was 1 molal with respect to NaCl.

A third set of experiments was run with 5-g samples of H-illite 35 (acid) using 25.00-ml portions of NaOH solutions (no salt). The tubes were stoppered with no. 7 polythene beakers and placed in a shaking table to equilibrate. After a minimum of 7 days in the shaking table, the tubes were centrifuged to a constant weight of clay cake. The supernatant liquid was analyzed for NaCl, if present, and for NaOH. The clays treated with NaCl were taken up as slurries, as described above, and analyzed for Cl^- ion uptake.

Uptake of NaCl by Na-Clays

Several 5-g samples of Na-illite no. 35 (resin) and Na-montmorillonite no. 31 (resin) were weighed into polythene tubes to which were added 25.00 ml of NaCl solution of various molalities. After equilibrium was reached on the shaking table, the clay samples were centrifuged to constant weight. Both the supernatant liquid and the clay cake in each tube were analyzed for Cl^- ion by the methods described above.

Centrifuging of Clays

The equilibrated clay samples were centrifuged in the 1×4 in. plastic tubes in an International Equipment Co. centrifuge (Clinical Model). Using 120 V D.C., a speed of 6500 rpm was attained. The distance between the center of the centrifuge and the center of the clay cake was 12.8 cm. The acceleration was thus almost 6000 g, sufficiently high to separate interstitial from " bound " water in the clay phase. A plot of time of centrifuging vs. weight of the wet clay showed a sharp decrease in weight in the first 5 min.

After 15 min, the curve was virtually flat, i.e. the loss in weight was then about 0.1 mg per 5 min. For the sake of uniformity, all samples were centrifuged for 30 min. The water uptake of the clays was calculated from the difference in weight between the centrifuged clay and the dry clay after correcting for the uptake of diffusible ions.

Clay Transference Numbers

Water and ion transference numbers in sodium clays equilibrated with NaCl solution were determined in the three-compartment transport cell shown in Fig. 4. The centrifuged clay sample was placed in the center compartment and the end compartments were filled with the saturating NaCl
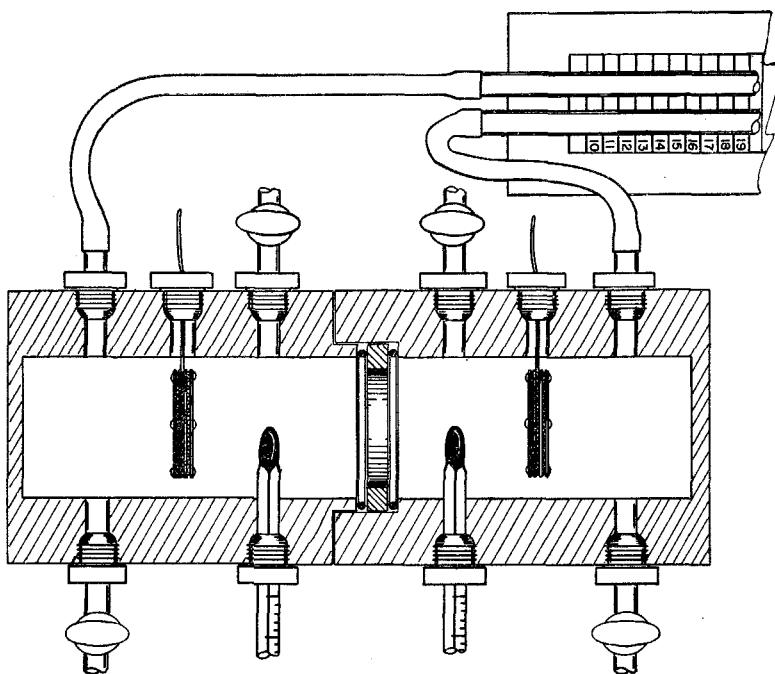

FIGURE 4.—Cell for determination of ion and water transference numbers.

solutions. A constant current from a coulometric power supply was passed between Ag/AgCl electrodes in the solution compartments. The increase in volume of the cathode compartment or decrease in anode volume was measured as a function of the faradays of electricity passed through the clay by noting the movement of liquid in the end compartment capillaries. Instantaneous values of t_w, the water transference number, were obtained

from the slopes of the plots of moles of water transferred vs. faradays of electricity. The chloride ion transference number, corrected for water transport, was found by analyzing the end compartments for Cl⁻ ion at the end of the run after completely draining the compartments. A full description of the cell is given elsewhere (Bernstein and Scala, 1959).

Equilibration Times

The length of time required to equilibrate the clay samples under given conditions was determined as follows: to two 20 g samples of H-illite were added respectively 200 ml of 0.2N NaOH and 200 ml of a solution which was 0.2N with respect to both NaOH and NaCl. To a third sample, 20 g of Na-illite, a 200 ml portion of 0.2N NaCl was added. The three samples were placed on a shaking table and periodically small samples of solution were withdrawn for analysis. The sodium clay came to equilibrium in four days. The H-illite samples required six days. The reaction went to 50 percent completion in 9 to 25 min.

EXPERIMENTAL RESULTS AND DISCUSSION
Titration of H-Clays

It becomes apparent in the study of hydrogen clays that the clay minerals behave as if they were weak polyacids. The specific volume of the centrifuged H-clay equilibrated with distilled water is very much smaller than the corresponding Na-clay. If the hydrogen clay were appreciably dissociated in water, the self-repulsion of the fixed negative charges would cause the matrix to expand. This effect would be particularly noticeable with a swelling clay. But the volume of a centrifuged sample of Na-montmorillonite increases over the dry clay volume by a factor of approximately 6 compared to a threefold increase for the hydrogen form. With illite, the volume of the sodium form increases by a factor of almost $2\frac{1}{2}$ compared to only a 50 percent increase for the hydrogen form. The weak acid behavior of these clays can be confirmed readily by preparing a slurry of homoionic Na-clay samples in distilled water. The pH of the supernatant liquid rose to 9 or 9.5, as shown in Table 1, indicating hydrolysis of the order of sodium acetate. Illite apparently hydrolyzes to a somewhat greater extent than montmorillonite, indicating a smaller apparent acid dissociation constant at room temperature. For comparison, the pH of the external phase in equilibrium with the polysulfonic acid IR–120–Na form was 6.5. The pH of the water was initially 6.2, and the increase of only 0.3 indicated virtually no hydrolysis. Further evidence of the weak acid characteristics of these clay minerals is shown in Table 2. Here, the drop in pH of the external NaCl solution is a measure of the hydrogen–sodium exchange. Only moderate exchange takes place with the hydrogen clays indicating the powerful competition of the clay exchange sites for the protons. Note that montmorillonite again is shown to be a somewhat stronger acid than illite by the lower pH value. With the strong-acid

polysulfonic resin IR–120–H, the exchange process is unhindered and the pH of the external solution falls to a small value.

The most obvious way to measure the acid strength of clays is to titrate the hydrogen forms. There are difficulties, however, in titrating these insoluble polyanions. Unlike a soluble acid system, the clay–water system

TABLE 1.—Na-CLAYS IN WATER

Clay	pH of Ext. Phase
Illite	9.5
Montmorillonite	9.0
IR-120	6.5

TABLE 2.—H-CLAYS IN 1.0 M NaCl

Clay	pH of Ext. Phase
Illite	3.45
Montmorillonite	2.77
IR-120	0.25

consists of two aqueous phases. The neutralization takes place in the internal phase while the pH can only be conveniently measured in the external phase. The sharp pH changes near the neutralization point are thus masked. Similarly, the buffer region for determination of the K_a, the apparent dissociation constant of the hydrogen clay, is also masked. However, the compositions of the two solution phases approach each other as the Donnan effect is swamped out. Thus the clay acid will behave as a soluble polymer if a large excess of neutral salt is added to the titration mixture. This effect is shown in Fig. 5 for the titration of H-montmorillonite in the presence and absence of NaCl. In the absence of NaCl, the inflection point is poorly defined, and, of course, the buffer region is completely masked. A well-defined titration curve is obtained, however, when the external phase is maintained at 1.0 m NaCl. An apparent dissociation constant of 10^{-4} is obtained, and the BEC value calculated from the inflection point agrees perfectly with the value obtained by the standard ammonium acetate method. It should be emphasized that in titration of an insoluble polyacid the composition (including pH) of the external solution is generally quite different from that of the internal phase. Thus the pK_a cannot be determined from the external pH in the absence of neutral salt. The addition of neutral salt swamps out the Donnan effect and the compositions of the two phases become nearly identical. However, the addition of neutral electrolyte will, in itself, cause an increase in K_a. With acetic acid, a simple weak acid, the

K_a increases with m_{NaCl}, passes through a maximum and then decreases. Thus the pK_a is 4.77 at $m_{NaCl} = 0$, 4.48 at $m_{NaCl} = 0.51$, and 4.74 at $m_{NaCl} = 3.01$ (Harned and Owen, 1958, p. 676). An increase in the K_a of soluble polyacids with addition of neutral salt has also been observed (Gregor, Luttinger and Loebl, 1955). Thus the K_a of a clay determined from the internal pH change (in the absence of salt) would probably be somewhat smaller than the K_a determined by the method described above.
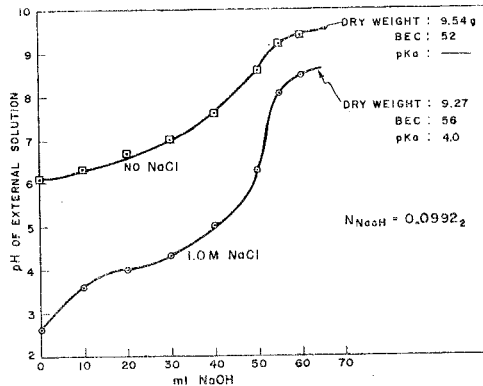
FIGURE 5.—Titration of H-montmorillonite no. 30a (acid) in water and in 1.0 m NaCl. BEC values calculated from inflection points.
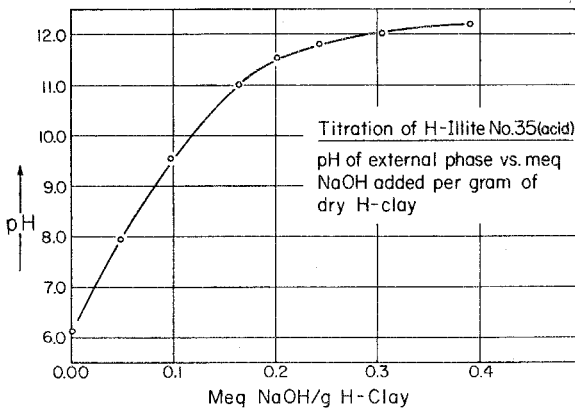
FIGURE 6.—Titration of H-illite no. 35 (acid) in water.

A titration curve for illite no. 35 (acid) is shown in Fig. 6. In the absence of NaCl, the inflection point fails to appear. This is further evidence that illite is a weaker acid than montmorillonite. However, if the external solution pH is plotted against the A value or the molality of the Na^+ ion in the clay

phase, as a measure of the degree of neutralization of the hydrogen clay, a well-defined inflection point does appear as shown in Fig. 7. The Na^+ ion molality was calculated as follows.
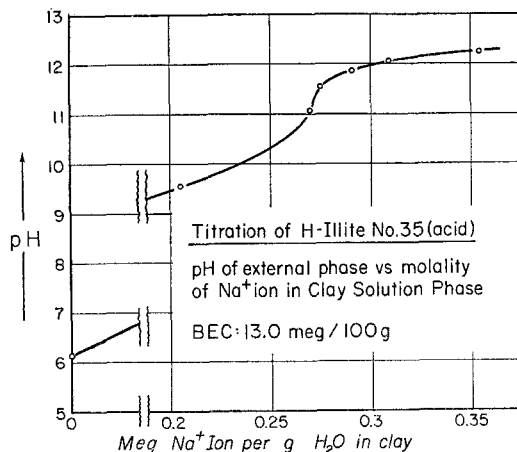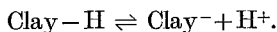

FIGURE 7.—Titration of H-illite no. 35 (acid) in water. pH of external solution plotted against Na^+ molality in clay phase.

The dissociation of a clay exchange group can be represented by

$$Clay - H \rightleftharpoons Clay^- + H^+.$$

Neglecting activity coefficients, the dissociation process can be expressed by the mass action law to give

$$K_a = \frac{A \cdot \bar{m}_H}{[Clay - H]} \tag{7}$$

where K_a, the apparent dissociation constant of the exchange group, has a value of about 10^{-4} for montmorillonite and is probably an order of magnitude lower for illite. The undissociated exchange group, represented by $Clay - H$, makes no contribution to the membrane activity and eq. (7) can be expressed in a form analogous to a solubility product, viz.

$$K_a = A \cdot \bar{m}_H \tag{7a}$$

Since K_a is small, A will be approximately equal to $\bar{m}_{Na}$ in the course of the titration. Then, making use of the water ionization product

$$\bar{m}_H \cdot \bar{m}_{OH} = 10^{-14}$$

$$K_a = \bar{m}_{Na} \cdot \frac{10^{-14}}{\bar{m}_{OH}}$$

or

$$\frac{\bar{m}_{Na}}{\bar{m}_{OH}} = K_a \times 10^{14}. \tag{8}$$

Thus the OH^- ion concentration in the clay phase is negligibly small before the clay is fully neutralized. The pH in the internal phase will be considerably lower than the external pH for the partially neutralized clay. Equating the chemical potentials of NaOH in the two phases (neglecting activity coefficients) gives

$$\bar{m}_{Na} \cdot \bar{m}_{OH} = m^2_{OH}. \tag{9}$$

Dividing equation (8) by (9) and again making use of the water ionization product gives

$$p\bar{H} = pH - 7 + \tfrac{1}{2}pK_a. \tag{10}$$

The internal pH of the partly neutralized clay is thus about 5 units lower than the external pH for montmorillonite and about 4.75 units lower for illite. The transfer of OH^- ion from the external to the internal phase results in the neutralization of a proton on the exchange site.

The internal Na^+ ion molality $\bar{m}_{Na}$ in the centrifuged clay as plotted in Fig. 7 is then given by

$$\frac{meq\ Na^+\ in\ clay}{g\ wet\ clay - g\ dry\ clay - 0.022\ (meq\ Na^+\ in\ clay)}$$

where 0.022 is the equivalent weight in g/meq of Na^+ corrected for the proton it replaces.

A plot of pH vs. A would give a curve identical to Fig. 7, except that the inflection would be sharper since A becomes progressively smaller than $\bar{m}_{Na}$ as the titration proceeds beyond the neutralization point. The BEC calculated from the titration curve agreed perfectly with the value found by the standard ammonium acetate method.

Fig. 8 is a plot of the pH of the external solution *vs.* meq of NaOH adsorbed per 100 g of clay in the titration of H-illite no. 35 (resin) in the presence of 1.0 molal NaCl. The BEC corresponding to the inflection point is 23 compared to 25 meq/100 g as found by the standard ammonium acetate method.

In summary, it is clear from the titration data that the clay minerals are weak acids, with illite somewhat weaker than montmorillonite. It is also clear that the acid behavior of the hydrogen clays cannot conveniently be characterized by standard titration techniques. Meaningful results can be obtained, however, by plotting the external pH against some function of the degree of neutralization of the internal clay phase. The internal solution changes can be determined directly by swamping out the Donnan effect with NaCl, or they can be calculated as shown above. It is also important to allow sufficient time for equilibration of the two phases between additions of titrant.

The important consequence of the weak acid behavior of these clays is that their membrane properties are strongly affected by pH. At low pH values, little membrane activity will be evident because of the intense competition of the exchange sites for hydrogen ion. The exchange sites are

completely dissociated and can exchange metal ions only when the pH of the equilibrating solution is high.

Anion Exclusion in Partly Neutralized Clays

The A value of a hydrogen clay, neglecting hydrolysis, is $K_a^{\frac{1}{2}}$, from eq. (7a). It would be expected then that the hydrogen clay would exhibit very little membrane activity in the hydrogen form. As shown above, the membrane activity increases as the clay is neutralized. Addition of further NaOH to the fully neutralized clay would then decrease the membrane activity because of anion leakage. These effects are summarized in Table 3, where the ratio $\bar{m}_{Cl}/m_{Cl}$ is tabulated for the clays, at various percentages of neutralization, in equilibrium with 1 molal NaCl solution.

Titration of H-Illite No.35 (resin)

pH of external phase vs. meq NaOH
absorbed per 100g of dry H-clay in
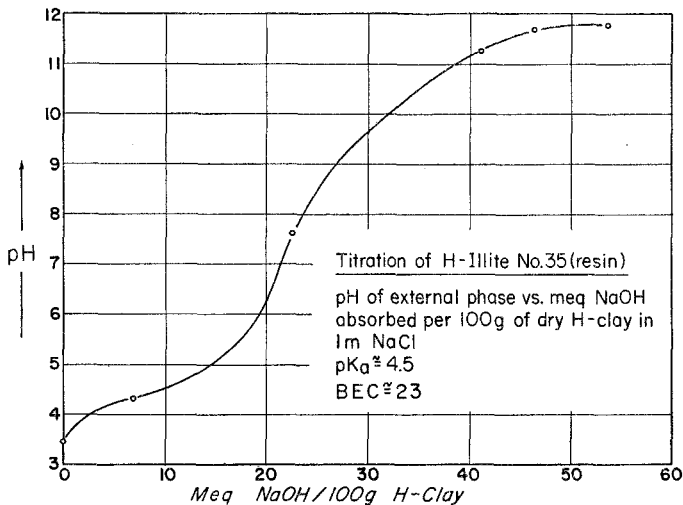1m NaCl
$pK_a \cong 4.5$
$BEC \cong 23$

FIGURE 8.—Titration of H-illite no. 35 (resin) in 1.0 molal NaCl. pH of external solution plotted against meq NaOH absorbed per 100 g of clay.

The ratio $\bar{m}_{Cl}/m_{Cl}$ is high even in the pure Na-Clays (100 percent neutralized). In fact, the value of 1 molal NaCl was chosen in order to swamp out the Donnan effect in the titration of the acid clays. Nevertheless, it is apparent, especially in montmorilolnite, that the membrane activity depends on the degree of neutralization. Undoubtedly, these effects would be more striking in more dilute NaCl solution.

Uptake of Water and NaCl by Na-Clays

In the sodium form the clay matrix is fully expanded when the clay is immersed in water. The membrane activity of the clay, however, depends on

the leakage of anions, which in turn is a function of the salinity of the saturating solution, as shown in eq. (5). The A value, which is directly related to the membrane activity of the clay, also varies with salinity owing to the variation of water uptake (swelling of the clay) with external phase NaCl concentration.

TABLE 3.—CHLORIDE ION LEAKAGE IN MOLAL NACL

Percent Neutralized	$(\bar{m}/m)_{Cl}$	
	Illite no. 35 (resin)	Montmorillonite no. 31 (resin)
0	0.957	0.943
31	0.945	—
100	0.940	0.895
182	0.949	—
186	—	0.937
206	0.956	—
219	—	0.944
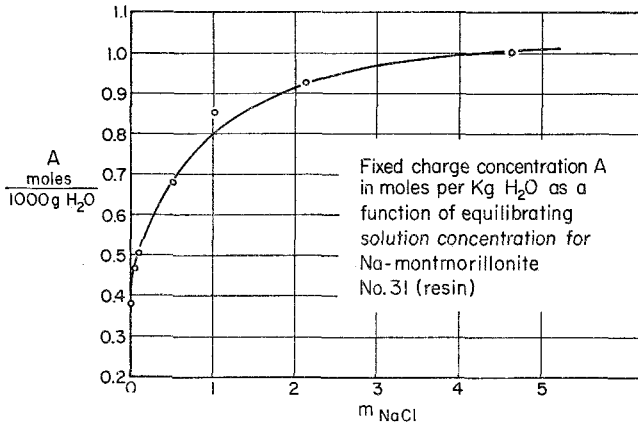
FIGURE 9.—Variation of the fixed charge concentration A with m_{NaCl} for Na-montmorillonite no. 31 (resin) where A is inversely proportional to the weight of water held by the clay.

The effect of salinity on the swelling properties of Na-montmorillonite no. 31 (resin) is shown in Fig. 9 where the A value is plotted as a function of the NaCl molality in the external phase. Since the BEC remains constant, the A value (which can be defined as BEC/g of water per 100 g of dry clay) is inversely proportional to the water uptake of the centrifuged clay. Essentially, therefore, Fig. 9 is a deswelling curve. The A value (or the deswelling)

increases very rapidly at low m_{NaCl} values and then more slowly at high salinities. At low m_{NaCl} values the leakage of anions is small and the activity of diffusible NaCl in the clay phase is low. The fixed negative charges exert their largest influence and the clay structure is fully expanded by electrostatic repulsion. The water content is high here and A is relatively low. With increase in m_{NaCl}, the concentration of Cl$^-$ in the clay increases and approaches Na$^+$ in the clay phase. The fixed charges become increasingly more shielded and ineffective, and the clay structure deswells. The phenomenon of deswelling has also been observed in consolidated clay-bearing rocks such as shaly sands. In some of these rocks, when the clay cements the grains, the deswelling of the clay will cause the entire structure to shrink.

The increase in A with increase in salinity partly compensates for the loss in membrane activity due to increased anion leakage. As a result, the loss of membrane activity with increase in salinity will be gradual rather than abrupt.
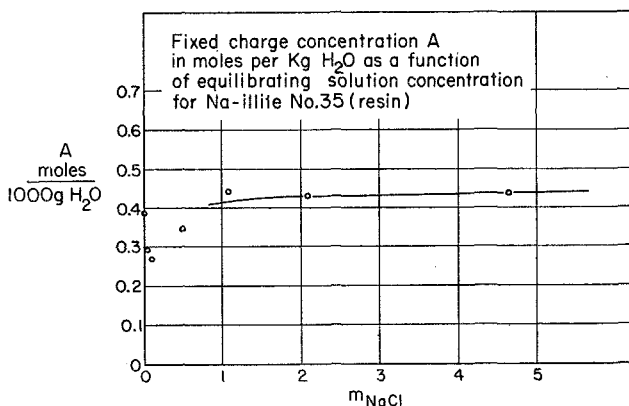

FIGURE 10.—Variation of the fixed charge concentration A with m_{NaCl} for Na-illite no. 35 (resin).

With Na-illite no. 35 (resin) which is relatively nonswelling, similar but smaller effects were found (Fig. 10). There are apparently some anomalous results in the low salinity range where the A value appears to go through a minimum before increasing in the expected manner. A possible explanation is that the potential of the double layer in the Na-clay does not reach its maximum value until the concentration of diffusible ions in the clay phase reaches a small but finite value. According to the Gouy concept of the diffuse double layer, the potential decreases with increase in the diffusible ion concentration. However, the Gouy theory implies that the double layer is not fully developed unless some diffusible ions are present. A minimum in the A value in the montmorillonite curve would also be expected if this explanation is valid, but it probably occurs at a m_{NaCl} value too low to detect.

10

The distribution of Na^+ and Cl^- ion between the clay and external solution phases for Na-montmorillonite no. 31 (resin) saturated with NaCl solution is shown in Fig. 11. Here, the ratio $\bar{m}_{Na}/m_{Na}$ is plotted on the right-hand ordinate against the NaCl molality in the external phase. The m_{NaCl} range is from 0.054 to 4.6 molal. The dashed line is the Na^+ ion uptake curve calculated from equation (5a), neglecting activity coefficients (taking $\bar{\gamma}\pm/\gamma\pm$ equal to unity). Equation (5a) predicts that $\bar{m}_{Na}$ generally will be greater
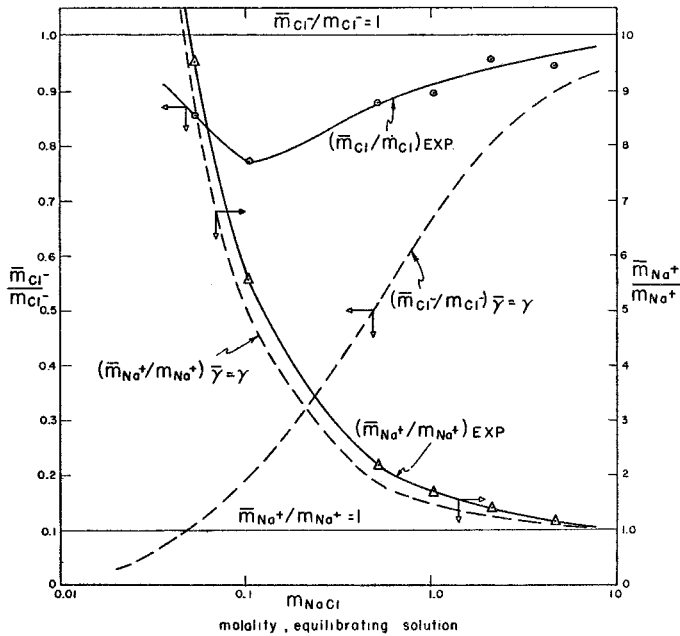
FIGURE 11.—The equilibrium distribution of Na^+ and Cl^- ion between Na-montmorillonite no. 31 (resin) and external NaCl solution as a function of m_{NaCl}. The dashed curves were calculated from equations (5) and (5a) taking $\bar{\gamma}/\gamma = 1$.

than m_{Na} and will approach m_{Na} at high salinities as the Donnan effect is progressively swamped out. The ratio $\bar{m}_{Na}/m_{Na}$ would appear to increase without limit as m_{Na} approaches zero, but actually it approaches a finite value because of hydrolysis (a Na-clay cannot be in true equilibrium with pure water). The Na^+ ion uptake is apparently normal, that is, the solid experimental curve lies fairly close to the theoretical curve. At high salinities, the curves begin to merge and both approach the limiting value of unity.

The chloride ion uptake is plotted as the ratio $\bar{m}_{Cl}/m_{Cl}$ on the left-hand ordinate in Fig. 11. Here, the ratio varies theoretically from zero to unity as

predicted by eq. (5). The striking feature here is the large discrepancy between the theoretical and experimental curves, particularly at low salinities. The clay is thus much more susceptible to leakage of anion than would be predicted from eq. (5). Another surprising feature is the minimum in the experimental chloride curve. From this curve, it would appear that at very low salinities, $\bar{m}_{Cl}$ might even be larger than m_{Cl}. Such effects have been observed in synthetic ion-exchange resins by Gregor and Gottlieb (1953) and other workers. Obviously, at low salinities, the mean activity coefficient ratio, $\bar{\gamma}\pm/\gamma\pm$, is much less than unity and cannot be neglected in predicting Cl^- ion uptake.
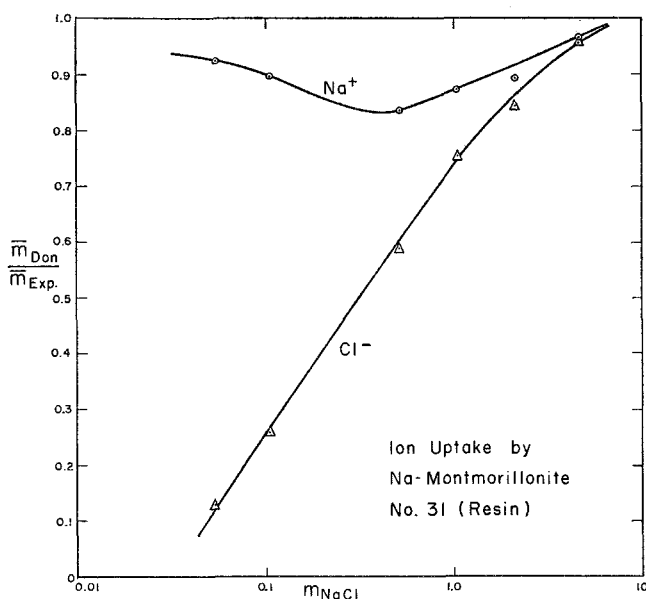

FIGURE 12.—Ion distribution data from Fig. 11 plotted as the ratio $\bar{m}_{Don}/\bar{m}_{Exp}$ against m_{NaCl}, where $\bar{m}_{Don}$ is the diffusible ion molality calculated from equations (5) and (5a) taking $\bar{\gamma}/\gamma = 1$, and $\bar{m}_{Exp}$ is the experimental diffusible ion molality.

In Fig. 12, the ion distribution in the same montmorillonite system is plotted as $\bar{m}_{Don}/\bar{m}_{exp}$ vs. m_{NaCl} where $\bar{m}_{Don}$ is the ion uptake predicted by eq. (5) and (5a). The deviations from ideality of the ion uptake are clearly shown. Extremely large deviations are evident in the Cl^- ion curve whereas the Na^+ ion deviation is small. As expected, in the high m_{NaCl} range, the curves begin to merge and approach the limiting value of unity.

The ion distribution between Na-illite no. 35 (resin) and the saturating NaCl solution is qualitatively the same, as shown in Fig. 13. However, the leakage of Cl^- ion is more regular and the minimum is not as pronounced.

The same results are plotted in Fig. 14 as $\bar{m}_{\text{Don}}/\bar{m}_{\text{exp}}$ *vs.* m_{NaCl}. Here again the deviation in Na$^+$ ion uptake is small compared to that of Cl$^-$ ion. One is thus tempted to assume that the single-ion activity of chloride in the clay phase is abnormally low compared to that of sodium. It is, of course impossible to compute single-ion activities from eq. (5) and (5a), but it is abundantly clear that the mean activity coefficient of diffusible NaCl is extremely low, particularly at low salinities.
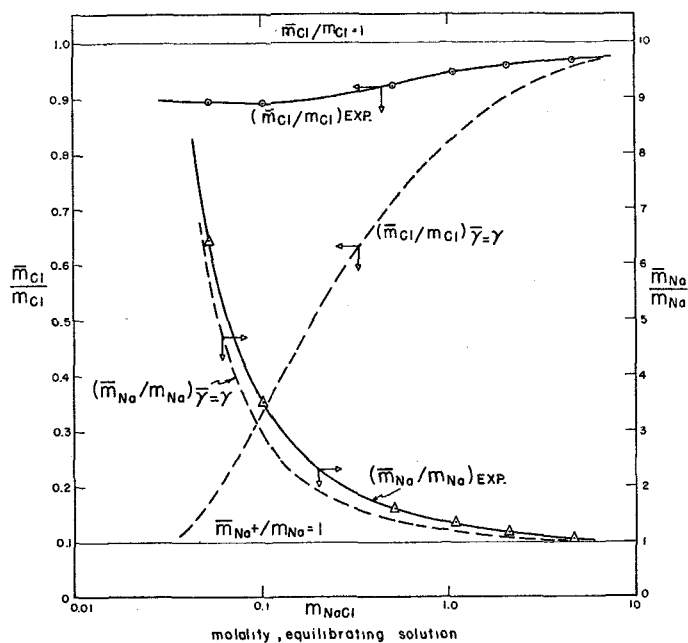
FIGURE 13.—The equilibrium distribution of Na$^+$ and Cl$^-$ ion between Na-illite no. 35 (resin) and external NaCl solution. See caption of Fig. 11 for details.

Knowing the A values and the molalities of the diffusible ions, the mean activity coefficients can be readily computed. These are plotted in Figs. 15 and 16 for the Na-montmorillonite no. 31 (resin) and Na-illite no. 35 (resin) systems, respectively. The $\gamma \pm_{\text{NaCl}}$ curve gives the variation of the mean activity coefficient of NaCl in the external phase (Harned and Owen, 1958, p. 735). The behavior of strong 1–1 electrolytes in aqueous solutions has been thoroughly studied (Harned and Owen, 1958, Chapter 12) and will not be discussed here at any length. The Debye–Hückel theory, based on the work required to separate the ions, predicts an increase in $\gamma \pm$ with dilution in the low concentration range, and $\gamma \pm$ to approach unity at infinite dilution; at high concentrations, interaction of the ions with the solvent leads to large

increases of $\gamma\pm$ with m_{NaCl}. The behavior of $\bar{\gamma}\pm$, on the other hand, is quite different in the lower m_{NaCl} range. Instead of approaching unity with increased dilution, $\bar{\gamma}\pm$ appears to approach zero or, at least, very low values.

Obviously, in the dilute range, the clay matrix is fully expanded and the counter Na^+ ions are strongly held in the double layer by the wall charges. Even though the Cl^- co-ion leakage is relatively high, there is a great preponderance of Na^+ in the clay phase (see Figs. 11 and 13) and the co-ions can
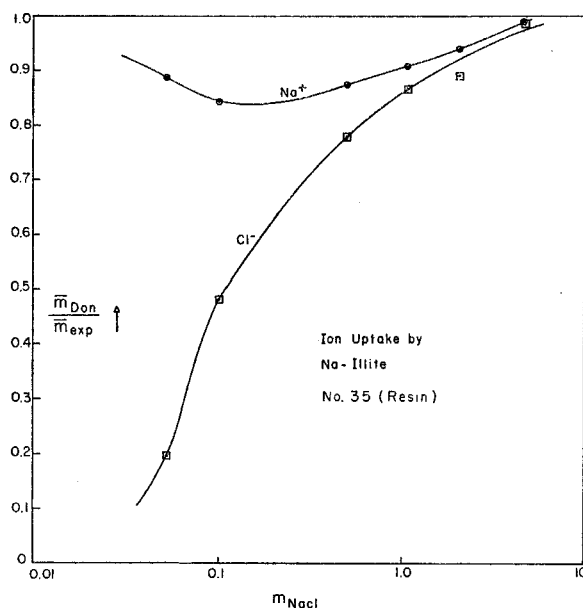
FIGURE 14.—Ion distribution data from Fig. 13 plotted as $\bar{m}_{\text{Don}}/\bar{m}_{\text{Exp}}$ against m_{NaCl}. See caption of Fig. 12 for details.

have relatively little effect on the wall charges. As a result, the activity coefficient of the Na^+ ions is lower than in free solution. A low activity coefficient for the Cl^- ions is also expected from the intense ion-cloud, resulting from the high concentration of Na^+ ions, surrounding the Cl^- ions on a time average. Kitchener has observed the same effects in synthetic ion-exchange resins (Kitchener, 1959, pp. 111–114).

As the concentration increases, the $\bar{\gamma}\pm$ curves go through a plateau and then begin to approach the $\gamma\pm$ curves. Obviously, as the double-layer influence becomes progressively swamped out, the clay acts only as a diluent to the internal solution phase and the curves begin to merge.

The reduced activity coefficient $(\bar{\gamma}\pm/\gamma\pm)_{\text{NaCl}}$ curves, Figs. 15 and 16, show the relationship between $\bar{\gamma}\pm$ and $\gamma\pm$ more clearly. These start at low

values in the dilute range and then approach unity in the concentrated range. Note that the montmorillonite curve is not as bowed as the illite curve. As expected, the fixed-charge effect persists to higher concentrations in montmorillonite.

The reduced activity coefficient $\bar{\gamma}\pm/\gamma\pm$ is directly related to the potential of the double layer, i.e. the ratio approaches unity as the double layer is swamped out, and it falls to low values when the double layer is fully developed. But according to the Gouy theory (Davies, 1958), the double-layer
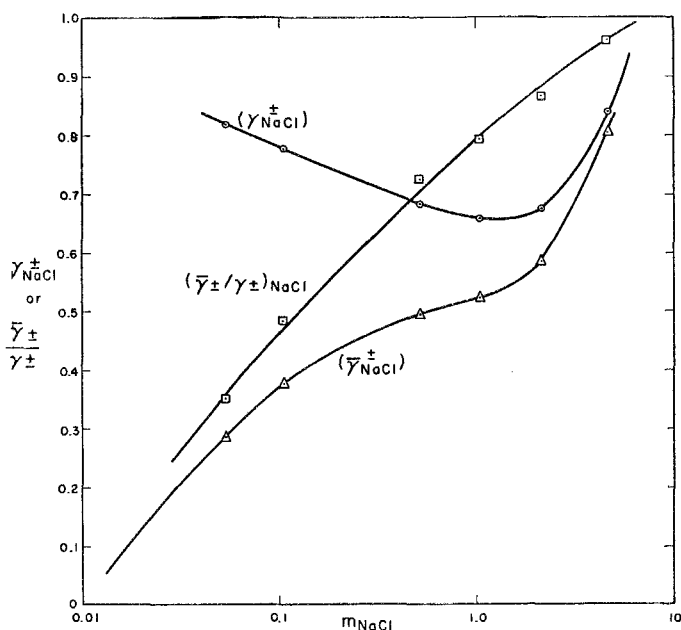
FIGURE 15.—Activity coefficients in the external solution $\gamma\pm$ and in the internal clay solution $\bar{\gamma}\pm$, and the reduced activity coefficient $\bar{\gamma}\pm/\gamma\pm$ as a function of m_{NaCl} for Na-montmorillonite no. 31 (resin).

potential is a logarithmic function of the leakage. The extent of leakage is conveniently expressed by the ratio $\bar{m}_{Na}/\bar{m}_{Cl}$. A linear relationship, independent of the clay type, is thus expected between $\bar{\gamma}\pm/\gamma\pm$ and log $\bar{m}_{Na}/\bar{m}_{Cl}$. Such a plot, for the two clays studied, is shown in Fig. 17. The linear relationship is closely followed down to $\bar{\gamma}\pm/\gamma\pm$ values of about 0.3. Gregor and Gottlieb (1953) observed similar effects in synthetic cation-exchangers.

The clay minerals, illite and montmorillonite, are efficient cation-exchangers when in the metal form (high pH) despite the abnormally high anion leakage at low salinities. The relatively high concentration of diffusible ions in the
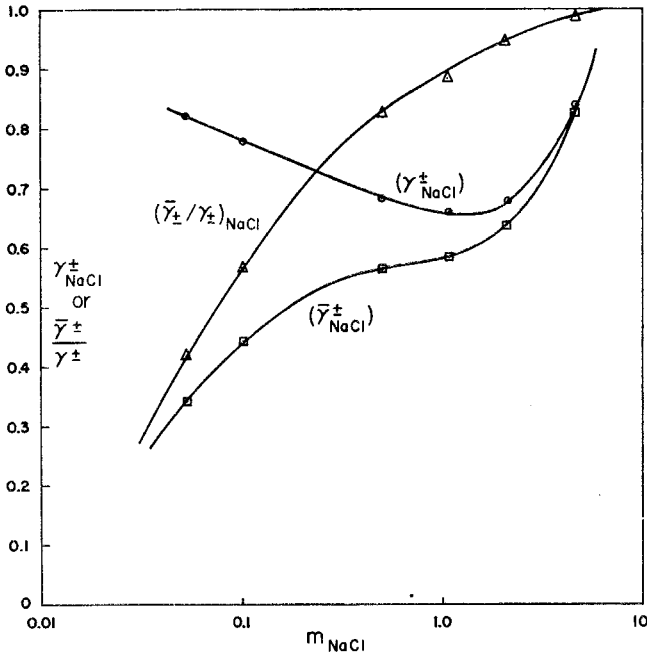
FIGURE 16.—Activity coefficients in the Na-illite no. 35 (resin)–NaCl solution system. See caption of Fig. 15 for details.
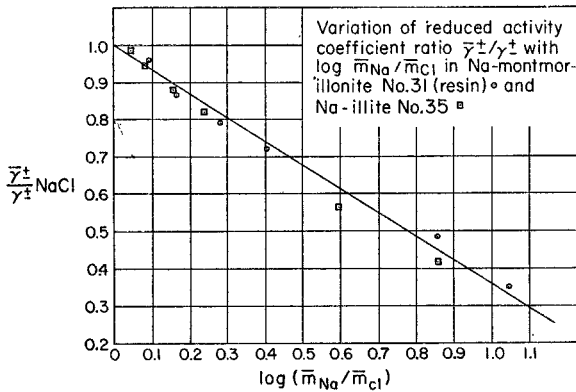

FIGURE 17.—Variation of the reduced activity coefficient ratio $\bar{\gamma} \pm / \gamma \pm$ with $\log_{10} \bar{m}_{Na} / \bar{m}_{Cl}$. The Na-montmorillonite no. 31 (resin) values are shown as circles. The Na-illite no. 35 (resin) values are shown as squares.

clay phase at low external concentrations is compensated for by the low activity of the internal phase ions. The abnormally low activity coefficients of the diffusible ions in the clay phase at low external solution salinity are a direct result of the clay phase double layer. In the dilute range, the double layer is fully developed as shown in the deswelling curves, Figs. 9 and 10. Sodium ions are strongly held in the double layer and while Cl^- ions are free to diffuse into the internal phase, their activity is low because of the high Na^+/Cl^- ratio.

At high salinities, the internal diffusible ion activity coefficients increase as the fixed charge effect is progressively swamped out. But the increased leakage is partly offset by the increase in A as the clays deswell.

Ion Transference Numbers

At 25°C, the potential in millivolts of the cell

$$NaCl\ (a_1)/Na\text{-}clay/NaCl\ (a_2)$$
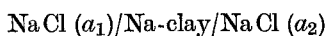
is given by

$$E = 59 \int_{a_1}^{a_2} (1 - 2\,t_{Na})d\,\log_{10} a_{NaCl} \tag{11}$$

where t_{Na} is the Na^+ ion transference number in the clay, i.e. the fraction of the current carried by the Na^+ ion through the clay. For the sake of simplicity, water transport has been neglected and the single ion activities in each of the two external phases have been set equal, viz.

$$a_{Na} = a_{Cl} = a_{NaCl}.$$

At low current densities, the current through the clay is carried only by Na^+ and Cl^- ion, so that $t_{Na} + t_{Cl} = 1$. If the clay behaves as an ideal membrane (no anion leakage), the current is carried only by Na^+ ion and eq. (11) reduces to eq. (6). On the other hand, if the Donnan effect is completely swamped out, t_{Na} approaches its free solution value of 0.4 and eq. (11) becomes

$$E = 11.8 \log \frac{a_2}{a_1}. \tag{12}$$

The transference number t_{Na} (or t_{Cl}) is thus a direct measure of the anion leakage and the membrane activity of the clay.

In the mud-filled borehole of an oil well, two electrochemical cells are in series as shown in Fig. 2:

$$NaCl(a_{mf})/Shale/NaCl(a_w)/liquid\ junction/NaCl(a_{mf}).$$
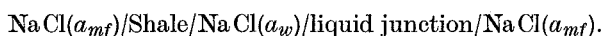
Applying eq. (11), assuming $t_{Na} = 1$ in the shale and $t_{Na} = 0.4$ in the liquid junction, gives

$$E_m = 59 \int_{a_{mf}}^{a_w} (1-2t_{Na})d \log a_{NaCl} = -59 \log \frac{a_w}{a_{mf}} \qquad (13)$$

$$E_{LJ} = 59 \int_{a_w}^{a_{mf}} (1-2t'_{Na})d \log a_{NaCl} = -12 \log \frac{a_w}{a_{mf}} \qquad (14)$$

$$E^1{}_{SP} = -71 \log \frac{a_w}{a_{mf}} \qquad (15)$$

The transference numbers in the clays are defined in terms of ion mobilities $\bar{u}$ by

$$t_{Cl} = \frac{\bar{m}_{Cl}\bar{u}_{Cl}/\bar{u}_{Na}}{\bar{m}_{Cl}\bar{u}_{Cl}/\bar{u}_{Na}+\bar{m}_{Na}} \qquad (16)$$

$$t_{Na} = \frac{\bar{m}_{Na}}{\bar{m}_{Cl}\bar{u}_{Cl}/\bar{u}_{Na}+\bar{m}_{Na}} \qquad (16a)$$

In Figs. 18 and 19, the chloride ion transference numbers in the two clays are plotted as functions of m_{NaCl}. The t_{Cl} values were computed from the experimental ion molalities and the free solution value of 1.5 for the mobility ratio $\bar{u}_{Cl}/\bar{u}_{Na}$, using eq. (16).

[1] If the potential across a permeable junction is measured with Ag/AgCl electrodes, the potential can be rigorously expressed in terms of mean ion activities without neglecting water transport to give

$$E = -118 \int_{a_1}^{a_2} (t_{Na}-0.018m_{NaCl} t_w)d \log a_{NaCl}$$

where t_w, the water transference number, is the moles of water transported through the permeable junction per faraday.

The electrochemical SP can also be expressed in terms of mean ion activities (Bernstein and Scala, 1959), as

$$E_{SP} = 118 \int_{a_{mf}}^{a_w} [(t'_{Na}-t_{Na}) - 0.018m_{NaCl}(t'_w-t_w)]d \log a_{NaCl}$$

where t' and t refer to the transference numbers through the liquid junction and shale, respectively.

Taking $t'_{Na} = 0.4$, $t_{Na} = 1$ and $t'_w = t_w = 0$, as above, gives

$$E_{SP} = -71 \log \frac{a_w}{a_{mf}}$$

From Figs. 18 and 19 it appears that the clays, particularly montmoril-lonite, are nearly perfect membranes at low salinities (provided the solution value of the mobility ratio in the clay phase is the same as in the solution phase). Both curves approach the limiting free solution value of 0.6 at high sal-inities, but still show considerable membrane activity at moderate concentra-tions.
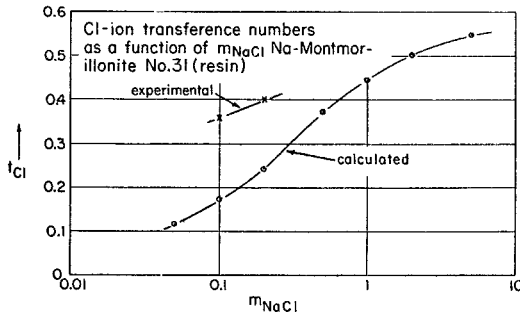

FIGURE 18.—The Cl⁻ ion transference number t_{Cl} as a function of m_{NaCl} in Na-montmoril-lonite no. 31(resin).
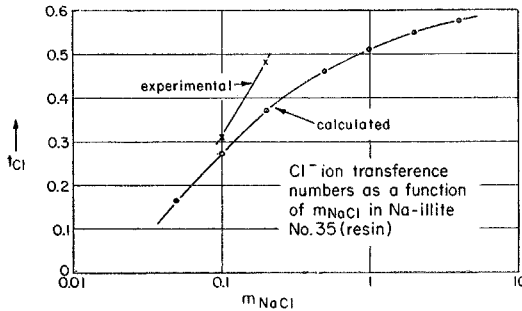

FIGURE 19.—The Cl⁻ ion transference number t_{Cl} as a function of m_{NaCl} in Na-illite no. 35 (resin).

Experimental ion transference numbers were determined with the cell shown in Fig. 4 for the two clays saturated with 0.1 and 0.2 molal NaCl. The two experimental points for each clay are also shown in Figs. 18 and 19.

Note that the experimental points are all higher than the corresponding calculated t_{Cl}'s. The obvious explanation is that the ratio $\bar{u}_{Cl}/\bar{u}_{Na}$ is higher in the clays than in free solution. Solving eq. (16) for the mobility ratio gives

$$\frac{\bar{u}_{Cl}}{\bar{u}_{Na}} = \frac{\bar{m}_{Na}t_{Cl}}{\bar{m}_{Cl}(1-t_{Cl})} \quad . \tag{17}$$

Table 4 gives the mobility ratio values calculated from the experimental ion transference numbers and molalities.

The high mobility ratio values (compared to 1.5 in free NaCl solution) are not surprising in view of the fact that the fixed charge effect is strong in this concentration range. The mobility of the sodium ion will be relatively low whereas the effect of the double layer on the chloride ion will be small. Similar effects have been observed in synthetic cation-exchange resins (Mackay and Meares, 1959). van Olphen and Waxman (1958) report a surface conductance of Na^+ ion in sodium bentonite that is only 55 percent of its value at infinite dilution. The fact that the mobility ratio is higher in montmorillonite than in illite is in agreement with the observed leakage and activity effects attributed to the higher fixed charge concentration in montmorillonite.

TABLE 4.—MOBILITY RATIOS IN CLAYS

	$\bar{u}_{Cl}/\bar{u}_{Na}$	
m_{NaCl}	Illite	Montmorillonite
0.1	1.81	4.14
0.2	2.28	3.15

The increase in the difference between the experimental and calculated transference numbers in illite (Fig. 19) with increase in concentration is difficult to explain. It would be expected that the internal mobility ratio would approach the free solution value as m_{NaCl} increases. The two t_{Cl} curves would then tend to merge.

There are, of course, insufficient experimental points to check this hypothesis. In montmorillonite, on the other hand, the mobility ratio does decrease with m_{NaCl}, in this limited range, and the experimental t_{Cl} curve appears to approach the curve of calculated t_{Cl} values (Fig. 18). In montmorillonite at least, the mobility ratio is another factor that tends to smooth out the membrane activity over the external solution concentration range. Thus, the increased leakage of anion with increase in m_{NaCl} is further compensated by the decrease in $\bar{u}_{Cl}/\bar{u}_{Na}$.

CONCLUSIONS

The clay minerals illite and montmorillonite exhibit weak acid characteristics. In aqueous solution, the clays form a two-phase solution system. In titrating the clays, typical weak acid curves are obtained by plotting internal solution composition changes against the external solution pH or by swamping out the Donnan effects with excess NaCl. At low pH values, the clays are poor ion exchangers because of the strong association of the exchange sites with hydrogen. They become efficient exchangers when converted to the sodium form at moderately high pH values. The membrane

efficiency correspondingly increases with increase in the degree of neutralization. The membrane activity falls off again with increase in external solution salinity due to anion leakage. At low salinities, anion leakage is abnormally high but the activity of the diffusible ions is very low. Increased anion leakage with increased salinity is partly compensated for by deswelling (increase in A value) and by the decrease in anion mobility in the clay phase relative to cation mobility.

A good knowledge of the electrochemical properties of the clay minerals is of extreme importance in oil-well log interpretation. The variation of ion mobilities with salinity will affect R_0, the resistivity of a water-saturated rock, if appreciable amounts of clay are present. In particular, the high ratio of internal to external solution concentration due to the Donnan effect, will cause the formation factor F (the ratio of rock resistivity to saturating fluid resistivity) to decrease if the saturating solution is dilute or becomes diluted as a result of invasion. Also, it is well known that the SP is depressed opposite clay-bearing sands because of the membrane properties of the clays. The effect of clay type and ion composition of the saturating fluid is thus important in improving interpretation of the SP log. Finally, a knowledge of the swelling properties of the clay minerals is important in the determination of effective porosities.

ACKNOWLEDGMENT

REFERENCES

Bernstein, F. and Scala, C. (1959) Some aspects of the streaming potential and the electrochemical SP in shales: *Amer. Inst. Mech. Engrs. Pet. Trans.*, v. 216., pp 465-468.

Davies, J. T. (1958) Monolayers of long-chain ions: in *Surface Phenomena in Chemistry and Biology*: Pergamon Press, New York, pp. 55–57.

Donnan, F. G. (1924) The theory of membrane equilibria: *Chem. Rev.*, v. 1, pp. 73–90.

Gregor, H. P. and Gottlieb, M. H. (1953) Studies on ion exchange resins. VIII. Activity coefficients of diffusible ions in various cation-exchange resins: *J. Amer. Chem. Soc.*, v. 75, pp. 3539–3543.

Gregor, H. P., Luttinger, L. B. and Loebl, E. M. (1955) Metal–polyelectrolyte complexes. I. The Polyacrylic acid–copper complex: *J. Phys. Chem.*, v. 59, pp. 34–39.

Harned, H. S. and Owen, B. B. (1958) *The Physical Chemistry of Electrolytic Solutions*: Reinhold Pub. Co., New York.

Kitchener, J. A. (1959) Physical chemistry of ion-exchange resins: in *Modern Aspects of Electrochemistry*, *No.* 2, Academic Press, Inc., New York.

Lewis, D. R. (1950) Base-exchange data: in *Analytical Data on Reference Clay Materials*, Preliminary Rept. no. 7, Reference Clay Minerals, A.P.I. Project 49, Columbia University, New York, pp. 91–124.

Mackay, D. and Meares, P. (1959) The electrical conductivity and electro-osmotic permeability of a cation-exchange resin: *Trans. Faraday Soc.*, v. 55, pp. 1221–1238.

Thompson, H. S. (1850) On the absorbent power of soils: *J. Roy. Agric. Soc.*, v. 11, pp. 68–74.

van Olphen, H. and Waxman, M. H. (1958) Surface conductance of sodium bentonite in water: in *Clays and Clay Minerals*, Natl. Acad. Sci.—Natl. Res. Council, pub. 566, pp. 61–80.

Way, J. T. (1850) On the power of soils to absorb manure: *J. Roy. Agric. Soc.*, v. 11, pp. 313–379.